Proceedings of the Twenty-sixth (2016) International Ocean and Polar Engineering Conference **www.isope.org**
Rhodes, Greece, June 26-July 1, 2016

ISBN 978-1-880653-88-3; ISSN 1098-6189

An Experimental Investigation of Freak Wave Forces on Vertical Cylinders

Yanfei Deng[a,b], Jianmin Yang [a,b*], Xin Li[a,b], Xinliang Tian[a,b]

[a]State Key Laboratory of Ocean Engineering, Shanghai Jiao Tong University
Shanghai, China
[b]Collaborative Innovation Center for Advanced Ship and Deep-Sea Exploration (CISSE)
Shanghai, China

ABSTRACT

An experimental investigation of the nonlinear wave forces on vertical cylinders induced by freak wave trains has been presented. A series of freak wave trains were modeled in a wave flume. The corresponding wave forces on vertical cylinders with different sizes were measured. The experimental wave forces were also compared with the Morison predictions adopting different stretch models. It shows that not only the strong asymmetric waves but also the weak asymmetric waves could result in strong asymmetric wave forces. The particle velocity distributions under the freak wave crest were measured with Particle Image Velocimetry (PIV) technique. It shows that the modified Wheeler model is capable to provide satisfactory predictions on the wave kinematics and wave forces of freak waves. By comparing the wave kinematics and wave forces results, it is concluded that the wave kinematics is the primary factors in predicting the strong asymmetric wave forces.

KEY WORDS: freak wave, vertical cylinder, wave forces, wave kinematics, Morison prediction

INTRODUCTION

Extreme waves have long been a major threat for the safety of marine structures and offshore workers. The extreme waves could result in significant wave run-ups, tremendous wave loads as well as the motion responses. Freak wave is one special appearance of extreme waves with abnormal wave height and asymmetrical wave profile. In recent decades, the reports on the damages and shipwrecks caused by freak waves emerge in an endless stream. By the statistics, there are more than 22 super carriers missing due to the attacks of freak waves between 1969 and 1994 (Kharif and Pelinovsky, 2003). Freak waves were observed at both deep sea and nearshore, in both stormy and calm seas (Chien et al., 2002; Mori et al., 2002). In view of this, interactions between freak waves and marine structures have been receiving more and more attention.

Since the formation of freak wave is often accompanied with a huge volume of water, rapid concentration of wave energy (Rudman and Cleary, 2013), it probably results in strongly nonlinear wave forces when rushing at marine structures. Cylindrical members are very common on offshore structures, and the wave forces on these structures have been widely studied. Among them, Morison formula (Morison et al., 1950) is the most famous and popular approach for predicting the wave forces on slender bodies. MacCamy and Fuchs (1954) presented the theoretical solution of linear diffraction problem for large diameter vertical cylinder. Kriebel (1998) studied the second-order wave forces on large diameter cylinders based on semi-analytical diffraction theory. In order to investigate the ringing phenomenon of marine structures in steep waves, multiple theories were proposed to calculate the third-order wave forces (Faltinsen et al., 1995; Malenica and Molin, 1995; Rainey, 1989). Being restricted by various kinds of assumptions, theoretical approaches are insufficient to predict the extreme wave loads due to freak waves.

Some experimental explorations have been performed to reveal the nonlinear characteristics of wave forces due to extreme waves. For example, Stansberg et al. (1995) investigated the wave forces on a vertical cylinder in extreme random wave and found that the high frequency components could contribute 10% to 20% to the peak forces. Chaplin et al. (1997) studied the wave forces under a series of single giant waves. It was concluded that the measured wave forces are higher than the Morison predictions and the discrepancies tend to increase with increasing wave steepness. Kim et al. (1997) proposed a new stretch model of wave kinematics for extreme waves, which was employed in studying the impact force of Draupner freak wave (Kim and Kim, 2003). Paulsen et al. (2013) investigated wave forces of extreme waves with experiments and CFD simulations. Artificial high frequency components of wave forces are observed in the measurements, which result from the impulsive unset of structural vibrations. Li et al. (2014) presented wave forces on a vertical cylinder in multi-directional focused waves and concluded that the spatial profile of the surface of multi-directional focused wave affects the wave forces. It is noted that wave forces under freak waves are strongly nonlinear and influenced by various factors. Available research provides us a preliminary understanding on the extreme wave forces, the knowledge on the nonlinear wave-structure interactions and the

* Corresponding author. Tel.: +86 021 3420750-2101.
E-mail address: jmyang@sjtu.edu.cn.

predictions of freak wave forces are still limited.

In this paper, we present an experimental investigation on the wave forces induced by a series of freak wave trains. To achieve better agreement with experimental results, different wave kinematics models are employed in the Morison predictions. The wave kinematics without structures were also measured with PIV technique and compared with the theoretical results. By analyzing the wave forces results combined with the wave kinematics results, the sources of extreme peak forces are recognized and conclusions on the freak wave forces are presented.

EXPERIMENTAL SET-UP

The experiments were carried out in the wave flume of State Key Laboratory of Ocean Engineering (SKLOE), Shanghai Jiao Tong University, China. The wave flume is 20.0 m long, 1.0 m wide and the water depth is d = 0.9 m. The wave trains were generated using a flap-type wavemaker. At the downstream of the wave flume, absorbing beach was used to eliminate the wave reflections.

In the experiments, the focal point as well as the cylinder location is set at 7.0 m away from the wavemaker. As shown in Fig.1, a total of 3 hollow aluminum cylinders with diameters D = 0.1 m, 0.15 m and 0.2 m were successively mounted on the rigid support frame. A six-component force transducer was installed between the cylinders and rigid support structures to measure the wave forces. The drafts of these cylinders are h = 0.3 m and distance between the transducer and the still water level (SWL) is l = 0.29 m. Besides, two cameras were also installed outside the glass wall to capture the freak wave kinematics when no cylinder structure exists.

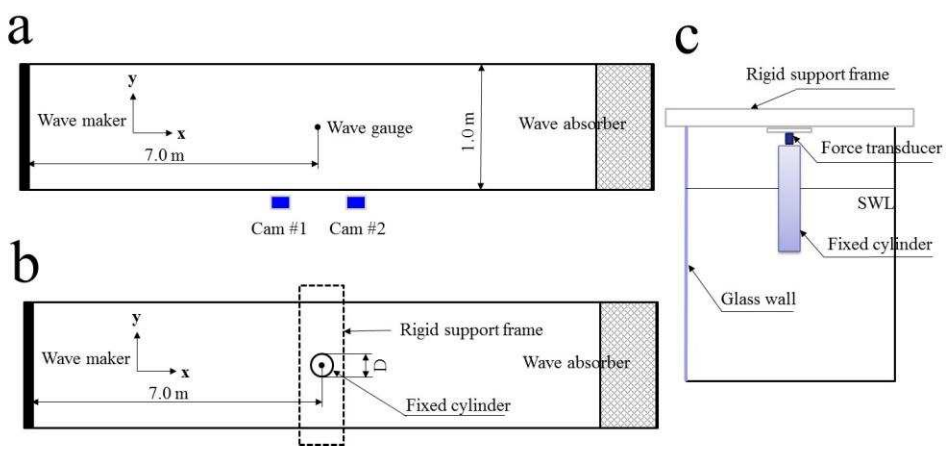

Fig.1 Arrangement for the measurement of wave forces

WAVE ENVIRONMENTS

A JONSWAP spectrum of the significant wave height H_s=0.11 m, peak period T_p=1.7 s and peakness factor γ=2.0 was used to design the target wave train with embedding model (Kriebel and Alsina, 2000). Fig.2 presents the target freak wave train computed from the above JONSWAP spectrum. The energy of transient wave accounts for 10.6% of the total and the remaining energy is for the random wave. The maximum wave height H_{max} is 0.2577 m and the crest height H_c is 0.18 m, leading to H_{max}/H_s=2.34 and H_c/H_s=1.64.

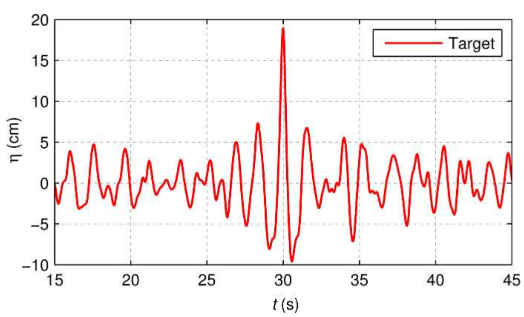

Fig.2 Target freak wave train

Four wave trains were then modeled and optimized with the phase-amplitude iteration scheme (Schmittner et al., 2009) in the wave flume prior to the wave force tests. These four waves are of similar wave profiles, and the wave elevations of three have been artificially adjusted to 40%, 60%, 80% of the original values. Fig.3 presents the generated freak wave trains, which were used to investigate the wave forces on vertical cylinders. These generated freak wave trains were measured using the wave probe at the target location x_c = 7.0 m, where the cylinders located in the formal tests.

STRONGLY ASYMMETRIC CHARACTERISITCS OF HORIZONTAL FORCES

The asymmetries of freak waves and the related horizontal forces could be inspected from the enlarged figures. According to Kim et al. (1997), the crest of a strong asymmetric wave has a distinct concave front and convex rear. The same is true for wave force analysis. Fig.4 and Fig.5 present the enlarged freak wave trains and the horizontal wave forces. The annotation “cvf” and “ccf” represent convex front and concave front, respectively. It can be seen from Fig.4 that, these four freak waves are with a crest that has a convex front and convex rear, or nearly straight front and convex rear. Thus, all the incident waves are weakly asymmetric. However, the cases are totally different for the wave forces. It shows in Fig.5 that the horizontal wave forces are with crests that have a concave front and a convex rear, or a concave front and a nearly straight rear. In this study, the wave forces induced by the weakly asymmetric freak waves are strongly asymmetric. This phenomenon somewhat disagrees with the views of Kim et al. (1997), which regards the strong asymmetric force as a consequence of strong asymmetric wave only.

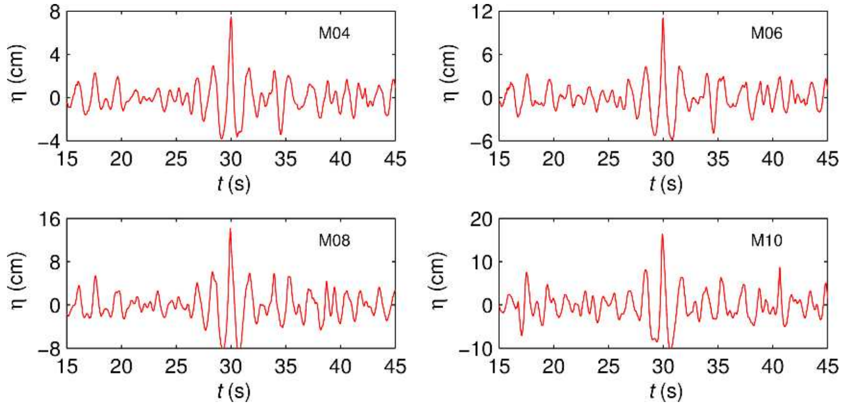

Fig.3 Generated freak wave trains

In Fig.5, it appears that the wave force profiles on different cylinders are similar for the same incident freak wave. The peak force is close to 35 N for wave M10, while it is less than 7 N for M04. It is evident that the wave force increases nonlinearly with wave height. With the increasing wave heights, the ratios between F_c and F_t, which represent wave force crest and the succeeding trough respectively, become larger from M04 to M10. Fig.6 shows the F_c/F_t values of the horizontal wave forces. Most of F_c/F_t values exceed 1.0 in various degree except the wave forces due to M04. The vertical asymmetry is more significant for wave forces on small diameter cylinders. Therefore, the viscous forces, which are proportional to the square of the flow velocity, may contribute to the peak forces. The maximum F_c/F_t value even reaches 2.96. It indicates that these wave forces are strongly nonlinear, and presents a challenge for the force predictions.

Fig.7 presents the dimensionless peak forces distributions. Similar to the above F_c/F_t values, the dimensionless peak forces are much larger for freak waves with large steepness, i.e. M10 cases. In this study, the influence of cylinder diameter on the dimensionless peak forces is not significant.

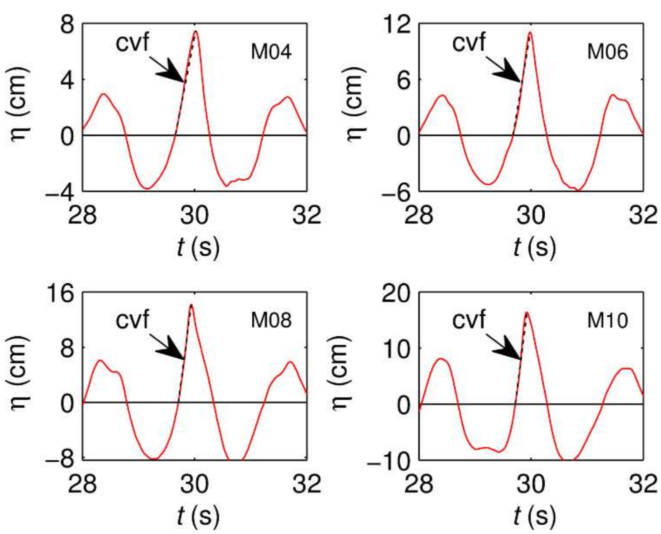

Fig.4 Enlarged freak wave trains

WAVE KINEMATICS OF FREAK WAVES

Accurate wave kinematics is essential for the wave force predictions based on Morison formula. Moreover, the wave kinematics are useful for wave breaking checking. The particle velocity profiles at focal position were measured with PIV technique. Since freak waves are with extremely high surface elevations, two stretch models are adopted to simulate the horizontal velocities in time domain.

In a modified Wheeler model (Wheeler, 1969), the wave elevation levels of long waves are regarded as the 'zero' level of short waves. The effective z coordinate z_e for i th wave component becomes

$$z_{e,i} = \frac{z - \varsigma_i}{1 + \frac{\varsigma_i}{h}} \tag{1}$$

where ζ_i is determined as follows

$$\varsigma_i = \sum_{j=1}^{i-1} A_j \cos(k_j x - \omega_j t + \theta_j) \tag{2}$$

To simulate the wave kinematics under transient wave group, Kim et al. (1997) proposed a stretching model given by

$$z_e = az^3 + bz^2 + cz + d \qquad (-h < z < H_c) \tag{3}$$

with

$$\begin{aligned}
a &= [(-h + H_c) + k(h + H_c)] / (h + H_c)^3 \\
b &= [-2(h^2 - hH_c + 2H_c) - k(h + H_c)(H_c - 2h)] / (h + H_c)^3 \\
c &= [H_c(H_c^2 - H_c h + 4h^2) + kh(h + H_c)(h - 2H_c)] / (h + H_c)^3 \\
d &= -\{h^2 H_c [k(h + H_c) + 2H_c]\} / (h + H_c)^3 \\
k &= (2.00 - \lambda) H_t / (H_c + H_t) \\
\lambda &= T_f / T_r
\end{aligned} \tag{4}$$

If $H_c / H_t \le 0$ then $\lambda = 1.0$, and if $\lambda > 1.95$, then $\lambda = 1.95$.

where H_c, H_t, T_r, T_f are respectively the wave crest, wave trough, crest rise time and crest fall time, and h is the water depth. Eq. (1) and Eq. (3) give the mapping relationship between the actual coordinate z and the effective coordinate z_e. By substituting the effective coordinate z_e into the following formula, we could easily obtain the simulated wave kinematics.

$$\begin{aligned}
u(x,z,t) &= \sum_i A_i \omega_i \frac{\cosh k_i(z+h)}{\sinh k_i h} \cos[k_i x - \omega_i t + \theta_i] \\
\partial u / \partial t(x,z,t) &= \sum_i A_i \omega_i^2 \frac{\cosh k_i(z+h)}{\sinh k_i h} \sin[k_i x - \omega_i t + \theta_i]
\end{aligned} \qquad (-h \le z \le 0) \tag{5}$$

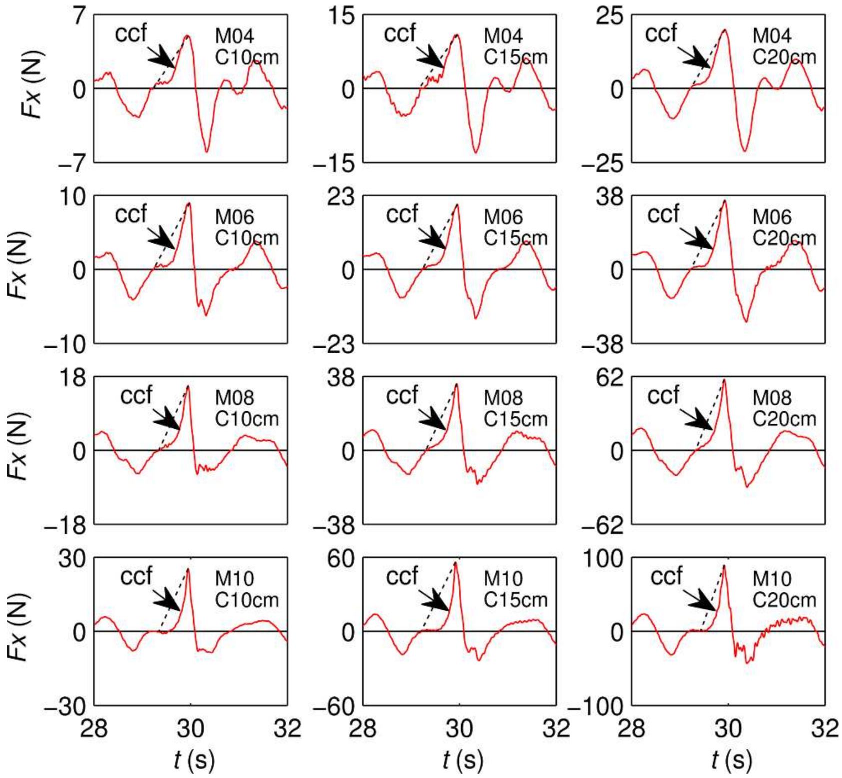

Fig.5 Enlarged horizontal forces due to freak waves

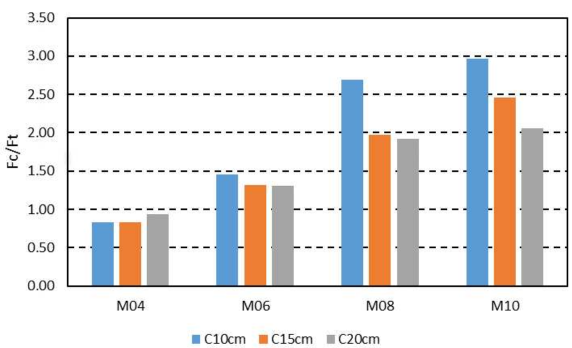

Fig.6 F_c/F_t distributions of wave forces

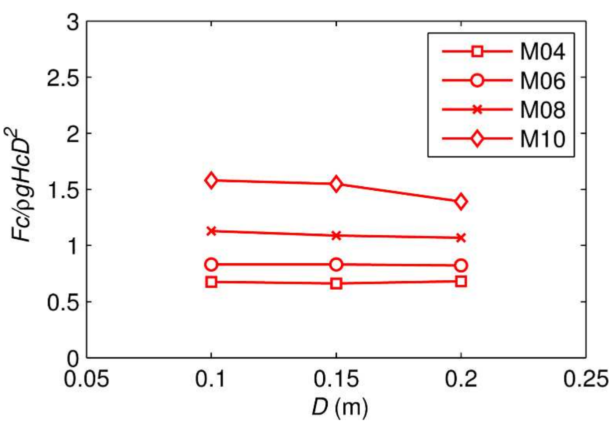

Fig.7 Dimensionless peak forces vs. cylinder diameter

Fig.8 shows the measured particle velocity distributions of freak wave M10 at the focal moment. Extreme horizontal velocities are observed at the crest of freak wave. The velocity variation at the crest is extraordinary large. It indicates that the wave kinematics distributions of freak waves could be highly nonlinear. The horizontal velocity profiles at focal moment and the moment 0.143 s after focusing are presented in Fig.9. Good agreements are observed between the measured values and predictions based on the modified Wheeler model apart from slightly deficiency at the wave crest. However, it seems that the predicted results given by Kim's model are considerably different from the experimental values. Compared with the measurements, the predicted horizontal velocities with Kim model are larger in most parts, and much smaller at the position near the free surface.

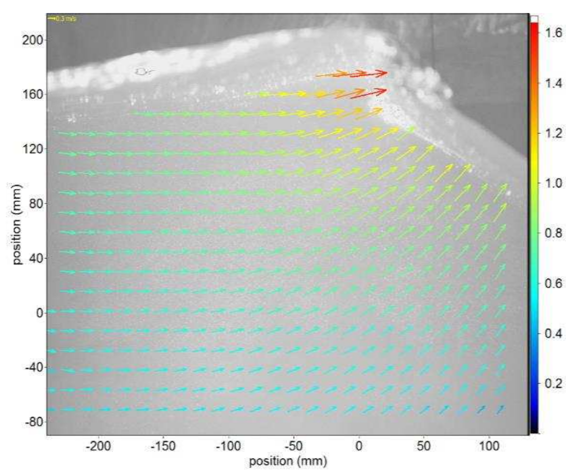

Fig.8 Particle velocity vector distributions of freak wave M10 at the focal moment from PIV meaurement.

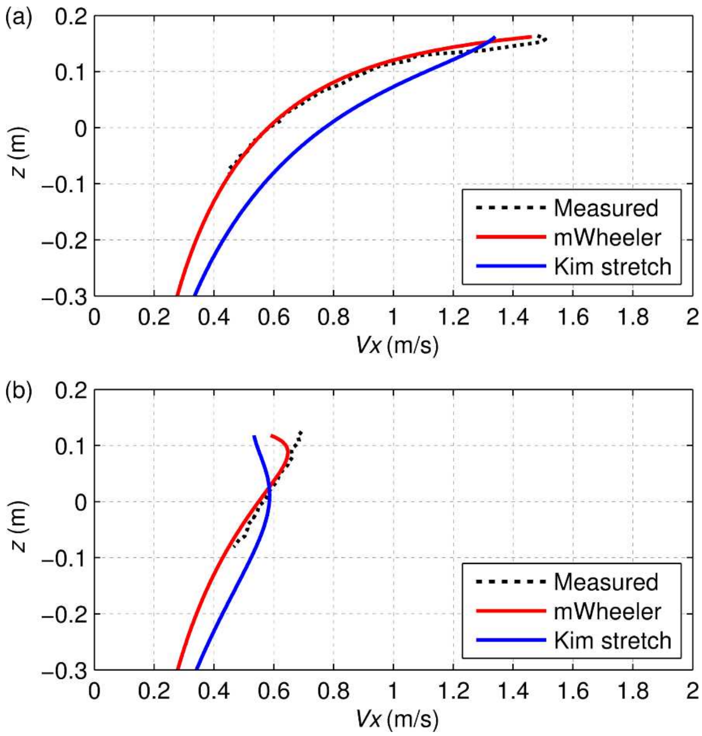

Fig.9 Particle velocity profiles of freak wave M10. (a) At the focal moment, (b) 0.143s after the focal moment.

MORISON PREDICTIONS

The wave trough-to-trough periods of the freak wave trains are about 1.43 s, leading to an equivalent wave length of 3.2 m. The D/L values vary from 0.031 to 0.063, which are among the slender body regime. The Morison formula (Morison et al., 1950) was thus used to calculate the horizontal forces. By adopting the above stretched wave kinematics, we could apply the following nonlinear form of Morison formula with integral from the cylinder bottom –v to the transient free surface level η(t).

$$F(t) = \rho C_M \frac{\pi}{4} D^2 \int_{-v}^{\eta} \frac{\partial u}{\partial t} dz + \frac{1}{2} \rho C_D D \int_{-v}^{\eta} u\left|u\right| dz \tag{6}$$

A constant inertial force coefficient C_M =2.0 and a constant drag force coefficient C_D =1.0 were employed in this study.

Fig.10 selects the wave forces on a cylinder of D=0.1 m as an example of the comparison between the measurement and the predictions with different wave kinematics models. It is observed that the predicted results are in general agreement with the measurements. The predicted value with Kim's stretch model overestimate the peak force due to freak wave, and the prediction with modified Wheeler model appears to underestimate it. For the other peak forces resulted from several high waves, the predictions based on Kim's model are also larger than the measurements while good agreements are observed between the predictions with modified Wheeler model and the measurements. Fig.11 shows the enlarged figures of wave forces from measurements and predictions. Similar situations are observed in other cases. This is in agreement with the above wave kinematics results. The exaggerated wave kinematics given by Kim's stretch model results in unreal large forces while the wave kinematics with much better consistency given by the modified Wheeler model produces relatively satisfactory results. The deficiency of the peak force with the modified Wheeler model may result from the underestimate of particle kinematics and the strongly nonlinear wave-structure interactions. Thus, the large wave kinematics is the primary factors for the strongly asymmetric wave forces. It is possible to achieve much better agreement of the peak forces if we put forward or update a better wave kinematics model for freak waves.

Fig.12 presents the ratios of the peak forces between the predicted and measured values. Also, better results are observed in the predictions with the modified Wheeler model. In addition, the predicted results get closer to the measurements for freak waves with small steepness, e.g. M04 and M06. The reason may be that the nonlinear wave-structure interactions for large-steepness freak waves are more significant.

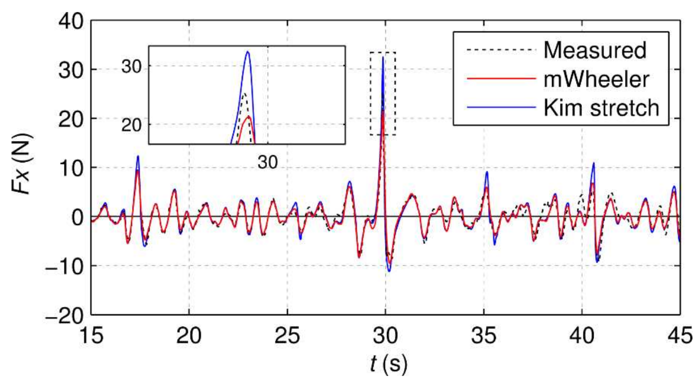

Fig.10 Comparison of horizontal forces on a cylinder of D=0.1 m induced by freak wave M10.

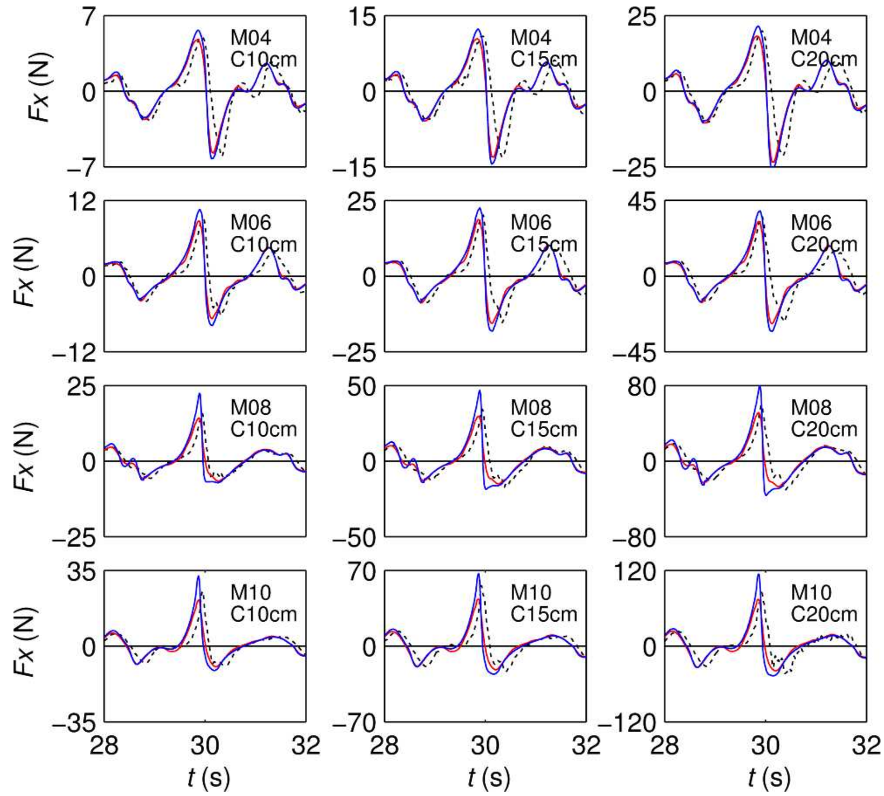

Fig.11 Enlarged figures of wave forces for comparisons. (The dashed lines, red lines and blue lines are respectively the results of measurements, mWheeler model, Kim model.)

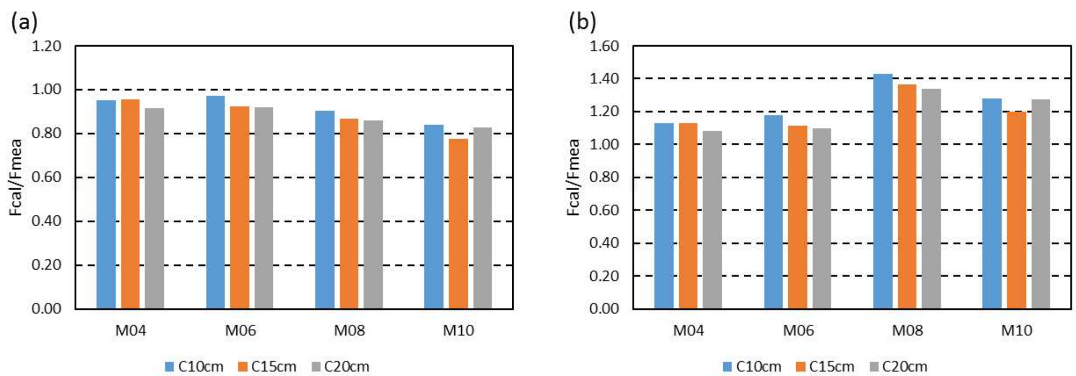

Fig.12 Comparisons of maximum horizontal forces between the predicted and measured results. (a) Modified Wheeler model; (b) Kim's stretch model.

CONCLUSIONS

For the sake of investigating the nonlinear horizontal forces induced by freak waves, we have performed a series of wave force tests with freak wave trains of different wave heights and vertical cylinders with different diameters. The asymmetric characteristics of both freak waves and wave forces are discussed. The wave kinematics as well as the wave forces are investigated by comparing with the results obtained with different wave kinematics models. The major conclusions are as follows.

（1） Strongly asymmetric wave forces are probably caused by weak asymmetric freak waves. Even the freak waves with steepness far below wave breaking limit could result in strongly asymmetric wave forces.

（2） The vertical asymmetric parameter F_c/F_t increases rapidly with increasing wave height and is more significant for the wave forces on the cylinder of small diameter.

（3） The wave kinematics predictions based on the modified Wheeler model agree well with the measurements except for the slight underestimate at the crest of freak wave, while the predictions of Kim's stretch model far overestimate the wave kinematics in most parts.

（4） Morison predictions with the modified Wheeler model provide satisfactory agreements with the measurements except for slight underestimation on the peak forces due to freak waves. The Kim's stretch model tends to overestimate the peak forces. The predicted results get closer to the measurements for freak waves with small steepness.

ACKNOWLEDGEMENTS

This work was financially supported by National Natural Science Foundation of China (Grant no. 51239007) and Shanghai Yang Fan Program (Grant no. 15YF1406100). These sources of support are gratefully acknowledged.

REFERENCES

Chaplin, J, Rainey, R, Yemm, R, (1997). “Ringing of a vertical cylinder in waves,” Journal of Fluid Mechanics, 350, 119-147.

Chien, H, Kao, C-C, Chuang, LZ, (2002). “On the characteristics of observed coastal freak waves,” Coastal engineering journal, 44 (04), 301-319.

Faltinsen, O, Newman, J, Vinje, T, (1995). “Nonlinear wave loads on a slender vertical cylinder,” Journal of Fluid Mechanics, 289, 179-198.

Kharif, C, Pelinovsky, E, (2003). “Physical mechanisms of the rogue wave phenomenon,” European Journal of Mechanics-B/Fluids, 22 (6), 603-634.

Kim, C, Xu, Y, Zou, J, (1997). “Impact and Nonimpact on Vertical Truncated Cylinder Due to Strong and Weak Asymmetric Wave,” International Journal of Offshore and Polar Engineering, 7 (03).

Kim, N, Kim, CH, (2003). “Simulation of Draupner freak wave impact force on a vertical truncated cylinder,” International Journal of Offshore and Polar Engineering, 13 (04), 260-265.

Kriebel, DL, (1998). “Nonlinear wave interaction with a vertical circular cylinder: wave forces,” Ocean Engineering, 25 (7), 597-605.

Kriebel, DL, Alsina, MV, (2000). “Simulation of extreme waves in a background random sea,” Proc 10th Int Offshore and Polar Eng Conf, Seattle, ISOPE, 31-37.

Li, J, Wang, Z, Liu, S, (2014). “Experimental study of interactions between multi-directional focused wave and vertical circular cylinder, part II: Wave force,” Coastal engineering, 83, 233-242.

MacCamy, RC, Fuchs, RA, (1954). “Wave forces on piles: A diffraction theory,” DTIC Document.

Malenica, Š, Molin, B, (1995). “Third-harmonic wave diffraction by a vertical cylinder,” Journal of Fluid Mechanics, 302, 203-229.

Mori, N, Liu, PC, Yasuda, T, (2002). “Analysis of freak wave measurements in the Sea of Japan,” Ocean Engineering, 29 (11), 1399-1414.

Morison, J, Johnson, J, Schaaf, S, (1950). “The force exerted by surface waves on piles,” Journal of Petroleum Technology, 2 (05), 149-154.

Paulsen, B, Bredmose, H, Bingham, H, (2013). “Focused wave impact on a vertical cylinder: Experiment, numerical reproduction and a note on higher harmonics,” IWWWFB28.

Rainey, R, (1989). “A new equation for calculating wave loads on offshore structures,” Journal of Fluid Mechanics, 204, 295-324.

Rudman, M, Cleary, PW, (2013). “Rogue wave impact on a tension leg platform: The effect of wave incidence angle and mooring line tension,” Ocean Engineering, 61 (0), 123-138.

Schmittner, C, Kosleck, S, Hennig, J, (2009). “A phase-amplitude iteration scheme for the optimization of deterministic wave sequences,” Proc 28th Int Conf on Ocean, Offshore and Arctic Eng, Hawaii, ASME, 653-660.

Stansberg, C, Huse, E, Krokstad, J, Lehn, E, (1995). “Experimental study of non-linear loads on vertical cylinders in steep random waves,” International Society of Offshore and Polar Engineers, Golden, CO (United States).

Wheeler, J, (1969). “Methods for calculating forces produced by irregular waves, Offshore Technology Conference,” Offshore Technology Conference, Dallas, Texas, USA, 71-79.